IN-02
40125

NASA Technical Memorandum 105223

p 14

Unsteady Flowfield of a Propfan at Takeoff Conditions

M. Nallasamy
Sverdrup Technology, Inc.
Lewis Research Center Group
Brook Park, Ohio

and

J.F. Groeneweg
National Aeronautics and Space Administration
Lewis Research Center
Cleveland, Ohio

Prepared for the
6th International Symposium on Unsteady Aerodynamics,
Aeroacoustics, and Aeroelasticity of Turbomachines and Propellers
sponsored by the International Union of Theoretical and Applied Mechanics
Notre Dame, Indiana, September 15-19, 1991

NASA

UNSTEADY FLOWFIELD OF A PROPFAN AT TAKEOFF CONDITIONS

M. Nallasamy
Sverdrup Technology, Inc.
Lewis Research Center Group
Brook Park, Ohio 44142

J. F. Groeneweg
National Aeronautics and Space Administration
Lewis Research Center
Cleveland, Ohio 44135

ABSTRACT

The unsteady flowfield of a propfan operating at takeoff conditions with angular inflow is examined by solving the three-dimensional Euler equations. The operating conditions considered are: Mach number = 0.31, advance ratio = 1.6 and inflow angle to the propfan =8.3°. The predicted results clearly show the cyclic variations of the blade power and thrust coefficients due to angular inflow. The flow changes from blade passage to passage are illustrated in terms of static pressure contours. The predicted blade surface pressure waveforms are compared with flight measurements. The predictions at the inboard radial station, r/R=0.68, show reasonable agreement with flight data. At the outboard radial station, r/R = 0.95, where the interactions of the tip vortex, the tip-region flow and the blade wake appear to result in a complex nonlinear measured response, the prediction shows poor agreement.

E-6540

INTRODUCTION

The advanced propfan design incorporates thin, highly loaded, highly swept blades to achieve superior performance at high speed over the conventional straight bladed propellers. These blades can produce a complex flowfield with leading edge/ tip vortices and or shock waves depending on the operating conditions. An understanding of the propfan flow features at the design and off-design operating conditions is crucial to the improvement of the design methodologies for future propfan designs. To aid this understanding, wind tunnel and flight tests have been conducted on a large-scale 9-ft (2.74 m) diameter SR7L propfan.

Steady and unsteady blade surface measurements were carried out on a two-bladed configuration in a transonic wind tunnel in Modane, France [1,2]. Flight tests of the eight bladed design configuration were done in two sets. In the first set called the Propfan Test Assessment (PTA) program detailed acoustic and structural measurements were taken [3]. In the second set called the PTA follow-on test detailed unsteady blade surface pressure measurements were done [4]. This is the first in-flight detailed blade surface pressure measurement on any advanced propfan. Thus we have an unique data base which may be used to understand propfan aerodynamic characteristics, validate prediction methods and to improve design methodologies.

For the flight tests, the propfan was installed on the left wing of a modified, instrumented Gulfstream II testbed aircraft. A nacelle tilt arrangement was used to vary the inflow angle to the propfan. The unsteady blade surface pressures were measured on a specially designed instrumented blade using 30 pressure transducers. The suction surface had 20 pressure transducers distributed over three radial stations (r/R = 0.68, 0.86 and 0.95, where r is the radial distance and R is the

blade tip radius) while the pressure surface had 10 transducers distributed over two radial stations (r/R=0.68 and 0.95).

The unsteady blade surface pressures were measured for three nacelle tilt angles, -3°, -1° (tilt down) and 2° (tilt up). The effective inflow angle, α, to the propfan, however, depends on the airplane angle of attack, nacelle tilt and upwash angle of the flow into the propfan. The propfan was tested over a wide range of inflow angles at takeoff and cruise operating conditions. The unsteady flowfield of a propfan at cruise operating conditions was examined by Nallasamy and Groeneweg [5]. In the present paper attention is directed to the unsteady flowfield of the propfan at takeoff conditions. The flow features are examined by obtaining the unsteady three-dimensional Euler solution. The predicted blade surface pressure waveforms are compared with flight measurements. This perhaps is the first time that such a comparison of predicted blade response with in-flight measurements has become feasible.

NUMERICAL SOLUTION

The unsteady three-dimensional Euler equations governing the inviscid flow through a propfan are solved employing a solution procedure developed by Whitfield et al. [6,7]. In this procedure, the equations in conservative differential form are transformed from a Cartesian reference frame to a time dependent body fitted curvilinear reference frame. The transformed equations are discretized employing a finite volume technique. An approximate Riemann solver is used for block interface flux definitions. A lower-upper (LU) implicit numerical scheme which possesses apparent unconditional stability is used to solve the discretized equations. The flowfield is represented by multiblock composite grids to limit the core memory requirements.

COMPUTATIONAL GRID

The configuration considered is that of the eight-bladed SR7L flight test. The direction of rotation of the propfan and the axes of reference are shown in Fig. 1. An H-grid is employed to represent the flowfield. Each blade passage is described by 107 by 41 by 13 (axial by radial by circumferencial) grid points and each passage is divided into three blocks with 107×41×5 grid points in each. Thus 24 blocks of grid describe the entire flowfield (8 blade passages) with 456,248 nodal points. Each blade surface is represented by 49 by 27 (chordwise by spanwise) grid points with higher resolution near the leading and trailing edges, the hub and the tip. This grid resolution was found sufficient to capture the leading edge vortex for the M = 0.2 and J = 0.88 case in [8]. Figures 2(a) and (b) show the bladewise surface and spanwise surface views of the grid, respectively. Figure 2(c) shows the distribution of the grid points on the blade surface and around it. The far-field boundary is three blade radii from the blade tip, the inflow plane is two blade radii upstream of the spinner and the exit plane is two blade radii behind the blade. These boundary locations have been found to be adequate to produce accurate results [9,10].

RESULTS AND DISCUSSION

The solution presented here is for the takeoff condition, Mach number, M = 0.31 and advance ratio, J = 1.6 (run = 40 and id = 3A in ref. 4). For this case, the nacelle tilt was -1° and the airplane angle of attack was 5.4°. In addition to these angles, the upwash angle at the propfan is needed to determine the effective inflow angle to the propfan. In the absence of a simple computational procedure to determine the upwash angle, an experimental correlation obtained by Heidelberg and Woodward [11] from their SR7A model propfan test in the NASA Lewis 9- by 15-ft wind tunnel, was used to estimate the inflow angle to the propfan. They first measured the pressure response of the blades as a function of inflow angle for the propfan alone configuration. Then the wing was installed downstream of the propfan (as in the flight test, tractor configuration) and blade pressure response was measured over a range of wing angles of attack and nacelle tilt. It is assumed that the local inflow angle and the propfan angle of attack are the same in the propfan alone case. Then by matching the measured first harmonic response of the blades with wing installation to that of propfan alone configuration, they found

the equivalent inflow angle as a function of wing angle of attack (Fig. 13 in [11]). This correlation was obtained for takeoff conditions, Mach number = 0.2 and advance ratio 0.88. The same correlation is used here to obtain the effective inflow angle to the propfan. For an airplane (wing) angle of attack of 5.4° and a nacelle tilt (droop) angle of -1° considered here, a value of 8.3° is obtained for the inflow angle from that correlation. Thus, the solution presented and discussed here was obtained with an inflow angle of 8.3° to the propfan axis (Fig. 1).

From an impulse start, the unsteady Euler solutions are obtained for three complete revolutions of the propeller to obtain a reasonably accurate solution. By the third revolution, the results have stabilized as indicated by the periodic variation of per blade power coefficient (Fig. 3(a)) during the second and third revolutions of the propfan. The figure shows the variation of the single blade power coefficient with azimuth angle for four blades, when started at ϕ_s = 0, 90, 180 and 270° respectively, for three complete revolutions of the propfan. The expected sinusoidal variation of the blade loading due to angular inflow is clearly observed in each case. The initial transient loading at the start of the run, however, is quite different for each blade and depends on the azimuthal position of the blade. Irrespective of the magnitude of this transient, the power coefficients become nearly sinusoidal at the end of the first revolution. The amplitude of the stabilished power coefficient during the third revolution varies +61 and -53 percent about the mean. The difference between the minimum and maximum levels about the mean results from the higher positive inflow angle that has been considered here, as a look at the velocity triangles would show. For low inflow angles the variation about the mean in the positive and negative directions has been found to be nearly the same [5,8]. Even though the inflow angle is higher than that in [8], the amplitude variation is small due the low Mach number of the flow considered here.

To see the harmonic content of the loading, the power coefficient for a single blade in the third cycle is Fourier transformed to yield $C_P = a_o + a_i \cos \omega t + b_i \sin \omega t$, where a_o, a_i, and b_i are the Fourier coefficients and t is the time. The predicted mean blade power coefficient, a_o, is 0.127 and is the same as that for the steady flow (α = 0). The mean power coefficient measured (per blade) in the flight test is 0.126 for the propfan operating conditions considered here. The loading spectrum is shown in Fig. 3(b). The loading is dominated by the first harmonic, but contributions do come from higher harmonics. The first harmonic loading lags the blade motion by 3.7°. This is much smaller than the 17.5° lag obtained for the takeoff conditions (M = 0.2 and J = 0.88, α = 3°) of the two-bladed configuration considered in [8]. It is due to the fact that the blade rotational frequency in the present case is only about half that of the case in [8], thus resulting in a low reduced frequency and flow unsteadiness. In addition, the two-bladed case showed the formation of a leading edge vortex which may have been partly responsible for the higher lag.

Figure 4(a) shows the spanwise variation of the elemental power coefficient for four azimuthal locations of the blade. Also shown in the figure is the curve for the steady flow (α = 0). It is seen that at ϕ = 0 and 90° azimuthal locations the blade loading is lower than the steady levels whereas at ϕ = 180 and 270° it is higher than the steady value. The magnitude of the cyclic variation of the loading depends on the spanwise location. The elemental thrust coefficient variations for the same four azimuthal locations and steady flow are shown in Fig. 4(b). It is seen that near the hub region, a small portion of the blade experiences negative thrust even in steady flow due to off-design operation of the propfan. The variations at different azimuth angles are similar to those of elemental power coefficient: at ϕ = 0 and 90° the values of the elemental thrust coefficient are less than the steady value while at ϕ = 180 and 270° the values are greater than the steady value. It is seen that in either case (Figs. 4(a) or (b)), the maximum deviation (in absolute value) from the steady value occurs at the radial station where elemental power/thrust coefficient attains a maximum, as would be expected from angle of attack variations.

The detailed flowfield information in the blade passages are presented in the form of static pressure contours at the spanwise station, r/R = 0.68, in Fig. 5. In a steady flow (zero degree inflow angle) the static pressure contours (shown on the top of the figure) in all the eight blade passages will be identical. But for an inflow angle of 8.3° changes in the flow occur from passage to passage. In the highly loaded portion of the revolution, the leading edge region near the pressure surface experiences higher pressure levels as indicated by the additional contours and levels (see blade passages marked 180-225, 225-270 and 270-315°). Of course, due to the low Mach number of the flow in the present case no passage shock forms as in the cruise case [3].

Next, we present detailed comparisons of the predicted blade pressure waveforms with flight data for two radial stations r/R = 0.68 and r/R = 0.95. In these waveform comparisons, 0° corresponds to the (top-dead-center) vertical direction for the aircraft installation, as in the presentation of flight data in [4]. First of all, it should be mentioned that during the flight tests no steady pressure measurements were made. However, some steady pressure data were obtained during the unsteady pressure test by retaining the DC component of the pressure signal. These data do not indicate the formation of a leading

edge vortex for the operating conditions, M = 0.31 and J = 1.6, chosen here. Consequently, the measured pressure waveforms on the suction surface at the outboard radial station do not show (see the discussion below for Fig. 8) the double hump nature observed in Modan tests [2] for M = 0.2 and J = 0.88.

Figure 6 shows the unsteady blade surface pressure as a function of azimuth angle for six transducer locations at r/R = 0.68, on the suction side. The measured and predicted blade responses indicate that the response is the largest at the transducer near the leading edge (x/c = 0.05, where x is the axial distance and c is the blade chord) and the response reduces gradually towards the trailing edge. The predicted phases of the waveform are in close agreement with the data. However, the amplitudes are overpredicted, the maximum overprediction occurring at the transducer near the leading edge. Similar agreements of the predicted waveforms with wind tunnel data at cruise conditions were also found in [12].

The pressure waveforms for the four transducer locations on the pressure side of the blade are shown in Fig. 7. Here again, the phases of the predicted waveforms agree quite well with flight measurements while the amplitudes are overpredicted. Thus the pressure waveforms for transducer locations at the inboard radial station on suction and pressure surfaces show reasonable agreement with flight data.

Figure 8 shows the pressure waveforms on the suction surface at r/R = 0.95 for the five transducer locations. Even at this radial station, the prediction indicates the largest response to occur near the leading edge and to reduce gradually towards the trailing edge. However, the flight measurements show that the highest response occurs downstream of the leading edge at x/c = 0.25. At this and other transducer locations downstream (x/c = 0.42, 0.58, and 0.92) we observe that the magnitudes are underpredicted and the measured pressure waveforms show a relative phase lag. The measured response at x/c = 0.25 is higher than the predicted one by as much as 100 percent at an azimuthal location of 300° which is in the lightly loaded (blade retreating) region of the revolution. Such a large response can only result from the movement of the tip vortex during the revolution and/or strong interactions between the tip vortex and tip-region flow which are not adequately resolved in the present solution. The phase difference between the waveforms may result from two things: (1) due to the interactions mentioned above and (2) the wing installation (or installation effect) in the flight tests as compared to propfan alone configuration of the computation. Heidelberg and Woodward [11] compare the measured pressure waveforms with and without wing for one transducer location, r/R = 0.75 and x/ c= 0.1 for α = 10°. They find that the waveforms are identical except for a small relative phase lag of 11° in the wing case. In the present case, the measured (wing case) waveforms also show a phase lag relative to the predicted (no wing) ones, which depends on the transducer location. The transducer near the leading edge (x/c = 0.08) show a small lead whereas all the remaining transducers show a phase lag ranging from 8 to 30°. More detailed investigation is necessary to understand the complex interactions in the tip region and the installation effects.

It should, however, be noted that when data indicated the formation of a leading edge vortex as in [2], the blade pressure response on the suction surface was double humped at all the transducer locations on the chord (at r/R = 0.91). The phases of the predicted wave forms were uncorrelated with measurements [8]. In the present case no such double hump response was measured, again perhaps indicating that no leading edge vortex forms at this operating condition.

Figure 9 shows the pressure waveforms for the six transducer locations on the pressure side of the blade at r/R = 0.95. The measured waveform at x/c = 0.58 is erratic for this run (=40) as noted in [4] and is not shown here. At the transducer locations x/c = 0.08, 0.25, 0.42 and 0.75 the predicted peak amplitudes agree reasonably well with flight data. At all the four locations the measured waveforms show a relative phase lag which again may be the result of wing/ no wing configurations and/or the tip-region flow being not resolved well in the predictions. The response at the transducer location x/c = 0.92 is small and the measured waveform is nearly 180° out of phase with the predicted one and with the wave forms at other four transducer locations. The transducer at x/c = 0.92 is not listed as erratic or inoperable. It is not clear as to the kind of blade wake-tip region interaction that will produce such a phase variation.

CONCLUDING REMARKS

Numerical solution of the flow through a propfan operating at takeoff conditions with angular inflow has been obtained. The results show that the blade power and thrust coefficients undergo cyclic variations due to angular inflow. The predicted blade surface pressure waveforms were compared with flight measurements. At the inboard radial station, r/R = 0.68, the

predicted pressure waveforms are in reasonable agreement with flight data. However, at the outboard radial station r/R = 0.95 the agreement between the measurement and prediction is poor. The discrepancies between the prediction and data at this radial station seem to arise due to inadequate flow resolution in the blade tip region. The installation effects may also contribute to the observed phase differences between the measured and predicted pressure waveforms.

REFERENCES

1. Bushnell, P.; Measurement of the Steady Surface Pressure Distribution on a Single Rotation Large-Scale Advanced Propfan Blade at Mach Numbers from 0.03 to 0.78. NASA-CR-182124, 1988.
2. Bushnell, P.; Gruber,M.; and Parzych, D.; Measurement of Unsteady Blade Surface Pressure on a Single Rotation Large Scale Advanced Propfan with Angular and Wake inflow at Mach Numbers from 0.02 to 0.70. NASA-CR-182123, 1988.
3. Little, B.H.; Poland, D.T.; Bartel, H.W.; Withers, C.C.; and Brown, P.C.; Propfan Test Assessment (PTA) Final Project Report, NASAS-CR-185138, 1989.
4. Parzych, D.; Boyd, L.; Meissner, W. and Wyrostek, A.; In Flight Measurement of Steady and Unsteady Blade Surface Pressure of a Single Rotation Large Scale advanced Propfan Installed on the PTA Aircraft, NASA-CR to be published, 1991.
5. Nallasamy, M; and Groeneweg, J.F.; Unsteady Euler Analysis of The flow Field of a Propfan at an Angle of Attack, AIAA-90-0339, also NASA-TM-102426, 1990.
6. Whitfield, D.L.; Swafford, I.W.; Janus, J.M.; Mulac, R.A.; and Belk, D.M.; Three Dimensional Unsteady Euler Solutions for Propfans and Counter-Rotating Propfans, AIAA paper 87-1197, June 1987.
7. Janus, J.M.; and Whitfield, D.L.; A Simple Time Accurate Turbomachinery Algorithm with Numerical Solutions of Uneven Blade Count Configuration, AIAA paper 89-0206, Jan. 1989.
8. Nallasamy, M.; and Groeneweg, J.F.; Unsteady Blade Surface Pressures on Large-Scale Advanced Propeller: Prediction and Data., AIAA paper 90-2402, also NASA-TM-103218, July 1990.
9. Nalllasamy, M.; Clark, B.J.; and Groeneweg, J.F.; Euler Analysis of the Three-Dimensional Flow Field of a High Speed Propeller: Boundary Condition Effects, Journal of Turbomachinery, Vol. 109, pp. 3332-339, 1987.
10. Nallasamy, M.; Yamamoto, O.; Warsi, S.; and Bober, L.J.; Large-Scale Advanced Propeller Blade Pressure Distributions: Prediction and Data, Journal of Propulsion and Power, Vol. 7, pp. 452-461, 1991.
11. Heidelberg, L.J.; and Woodward, R.P.; Advanced Turboprop Wing Installation Effects Measured by Unsteady Blade Pressure and Noise, AIAA paper 87-2719, also NASA-TM-100200, 1987.
12. Heidelberg, L. J.; and Nallasamy, M.; Unsteady Blade Pressure Measurements for the SR-7A Propeller at Cruise Conditions, AIAA paper 90-4022, Oct. 1990, also NASA-TM-103606.

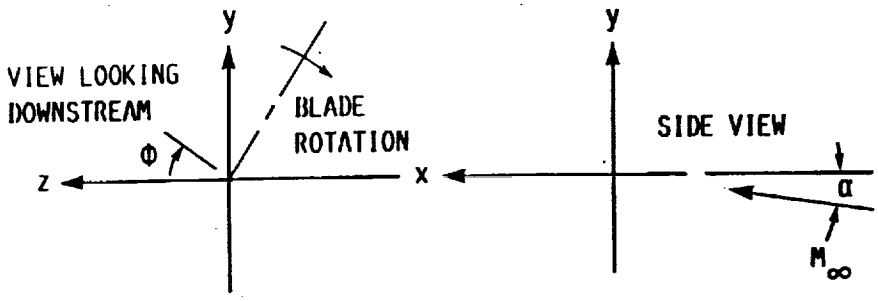

Figure 1. – Axes of reference.

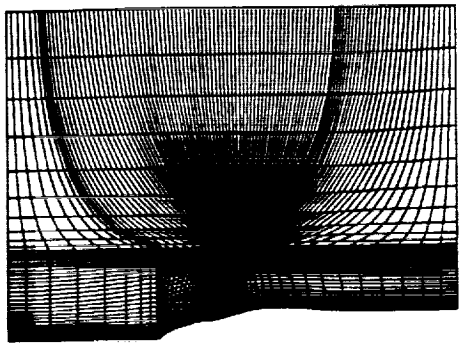

(a) Bladewise surface.

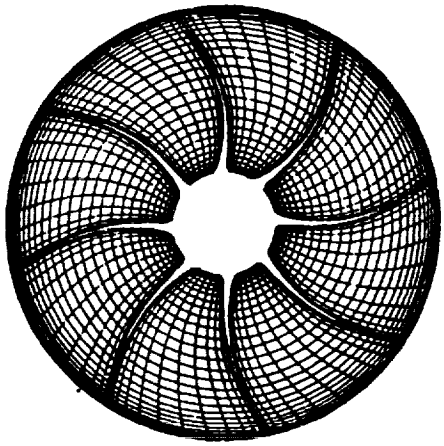

(b) Spanwise surface.

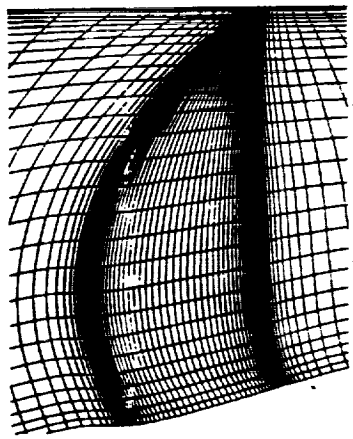

(c) Distribution of grid points on and near the blade surface.

Figure 2. – Computational grid.

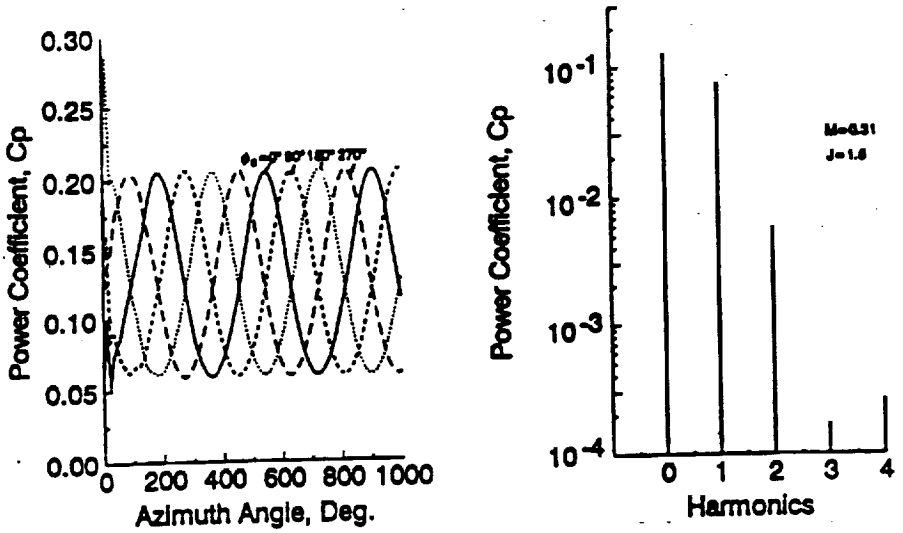

(a) Power.

(b) Loading spectrum.

Figure 3.—Power per blade variation.

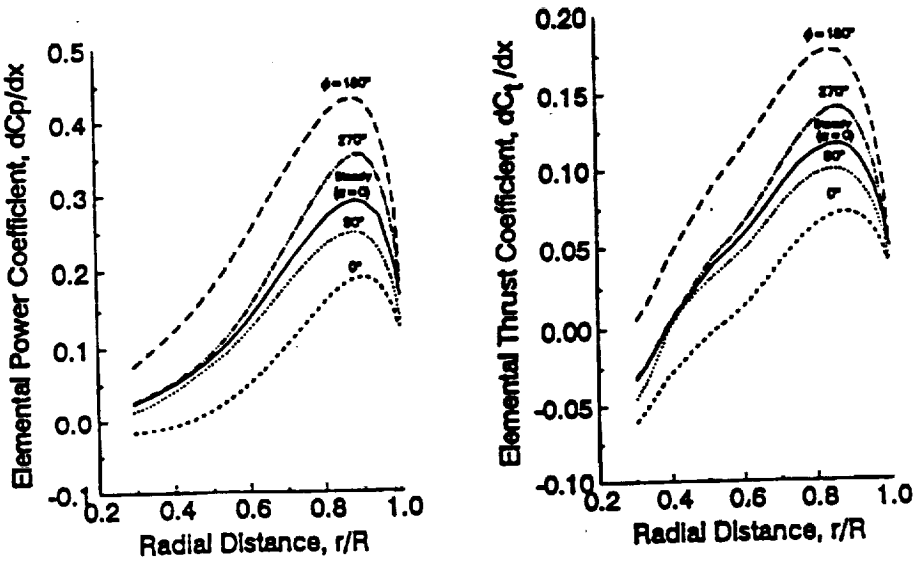

(a) Power.

(b) Thrust.

Figure 4. – Elemental Power and thrust coefficient.

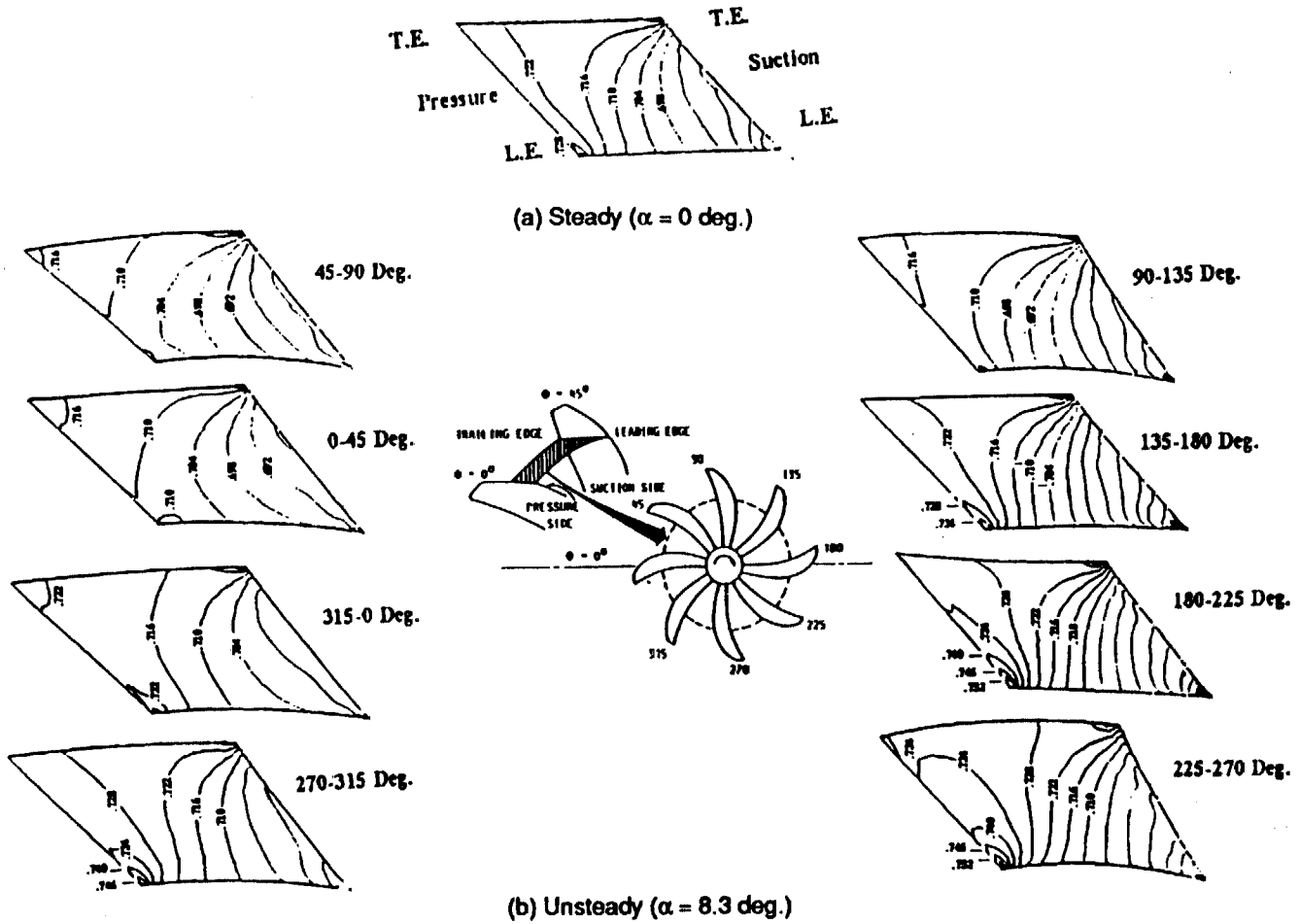

Figure 5. – Instantaneous static pressure contours in the blade passages at r/R=0.68. M=0.31, J=1.6.

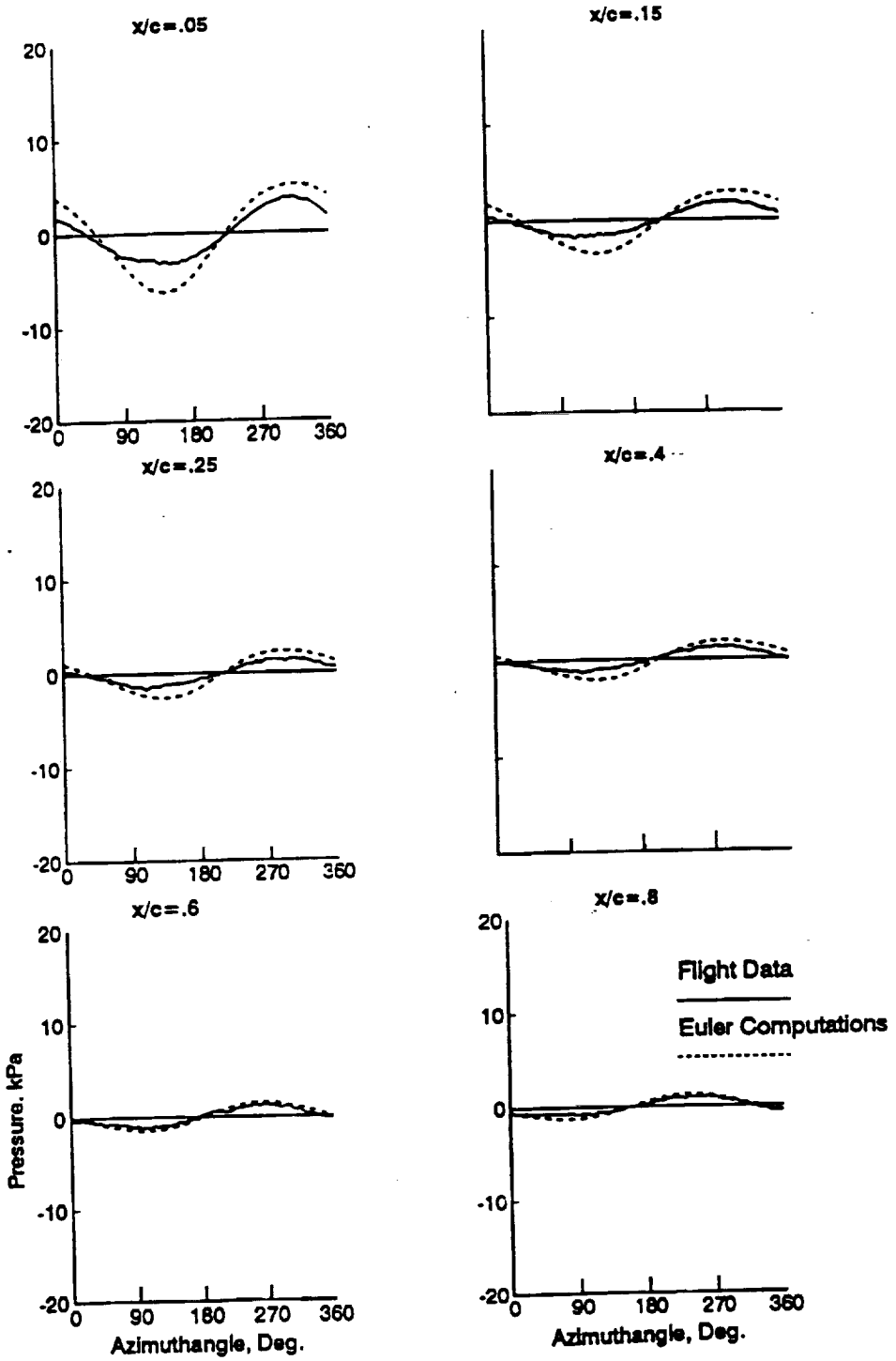

Figure 6. – Predicted and measured presure waveforms at r/R=0.68 on the suction surface. M=0.31, J=1.6, α =8.3°.

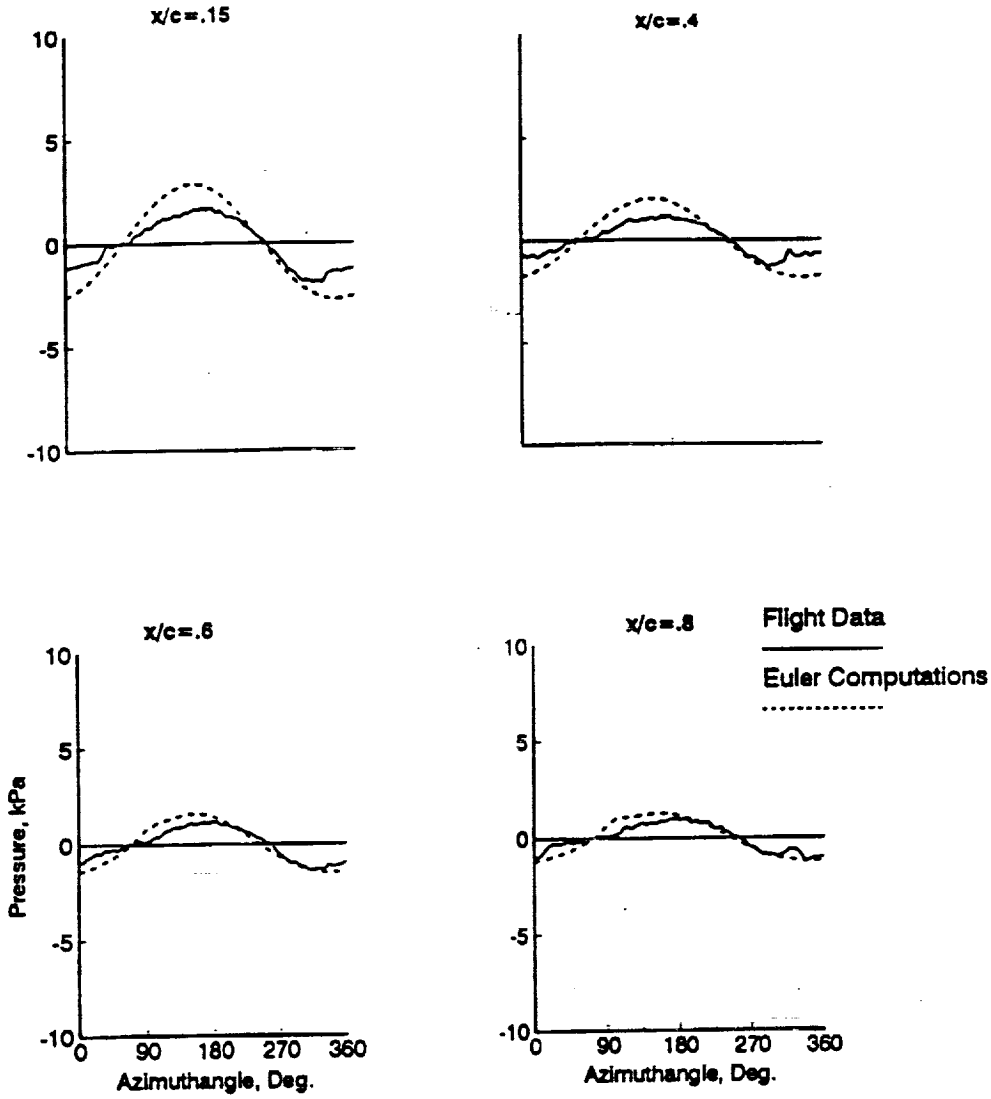

Figure 7. – Predicted and measured presure waveforms at r/R=0.68 on the presure surface. M=0.31, J=1.6, α =8.3°.

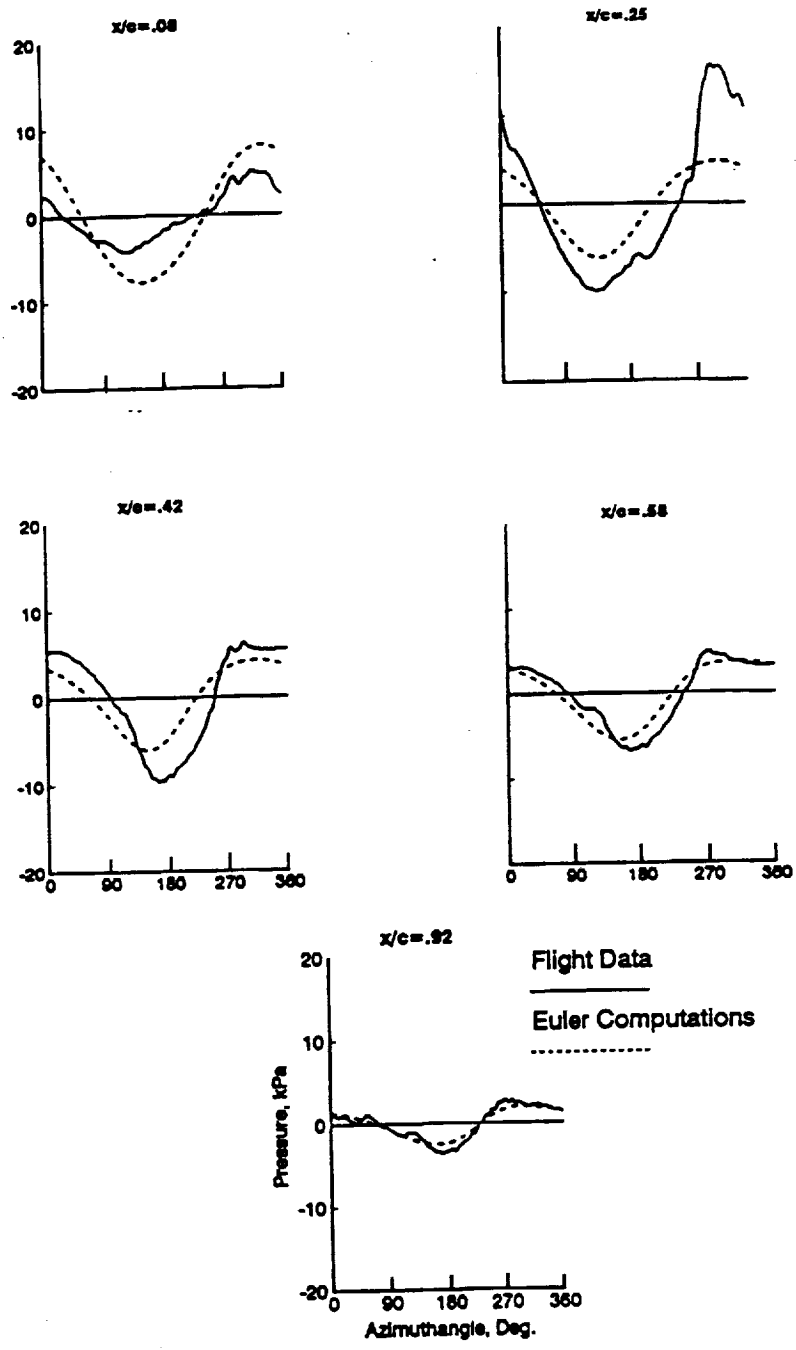

Figure 8. – Predicted and measured presure waveforms at r/R =0.95 on the suction surface. M=0.31, J=1.6, α =8.3°.

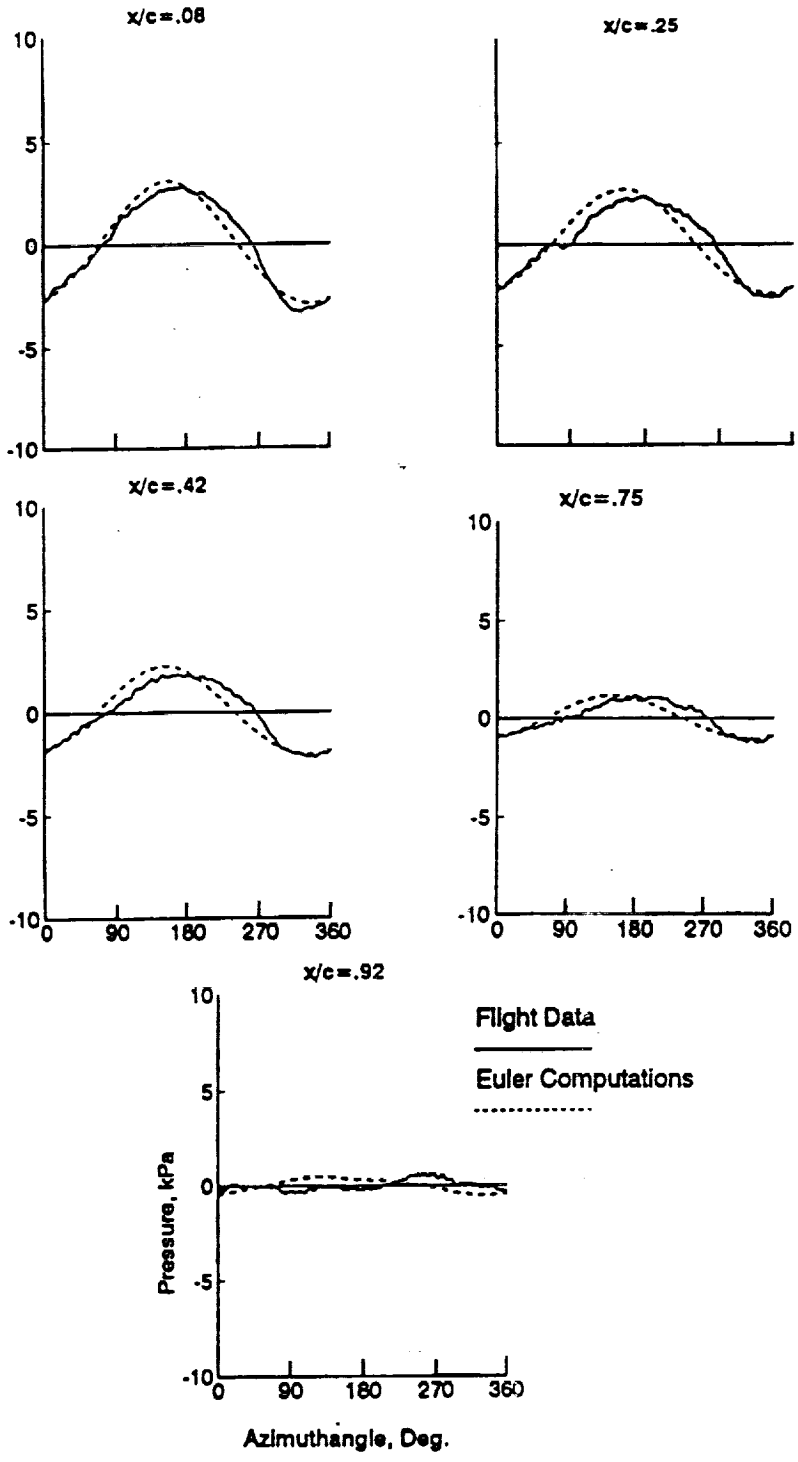

Figure 9. – Predicted and measured presure waveforms at r/R =0.95 on the presure surface. M=0.31, J=1.6, α =8.3°.

REPORT DOCUMENTATION PAGE

Form Approved
OMB No. 0704-0188

1. AGENCY USE ONLY (Leave blank)	2. REPORT DATE	3. REPORT TYPE AND DATES COVERED
		Technical Memorandum

4. TITLE AND SUBTITLE
Unsteady Flowfield of a Propfan at Takeoff Conditions

5. FUNDING NUMBERS
WU-535-03-10

6. AUTHOR(S)
M. Nallasamy and J.F. Groeneweg

7. PERFORMING ORGANIZATION NAME(S) AND ADDRESS(ES)
National Aeronautics and Space Administration
Lewis Research Center
Cleveland, Ohio 44135-3191

8. PERFORMING ORGANIZATION REPORT NUMBER
E-6540

9. SPONSORING/MONITORING AGENCY NAMES(S) AND ADDRESS(ES)
National Aeronautics and Space Administration
Washington, D.C. 20546-0001

10. SPONSORING/MONITORING AGENCY REPORT NUMBER
NASA TM-105223

11. SUPPLEMENTARY NOTES
Prepared for the 6th International Symposium on Unsteady Aerodynamics, Aeroacoustics and Aeroelasticity of Turbomachines and Propellers sponsored by the International Union of Theoretical and Applied Mechanics, Notre Dame, Indiana, September 15-19, 1991. M. Nallasamy, Sverdrup Technology, Inc., Lewis Research Center Group, 2001 Aerospace Parkway, Brook Park, Ohio 44142 (work funded by NASA Contract NAS3-25266). J.F. Groeneweg, NASA Lewis Research Center. Responsible person, M. Nallasamy, (216) 826-6631.

12a. DISTRIBUTION/AVAILABILITY STATEMENT
Unclassified - Unlimited
Subject Categories 71 and 02

12b. DISTRIBUTION CODE

13. ABSTRACT *(Maximum 200 words)*

The unsteady flowfield of a propfan operating at takeoff conditions with angular inflow is examined by solving the three-dimensional Euler equations. The operating conditions considered are: Mach number = 0.31, advance ratio =1.6 and inflow angle to the propfan =8.3°. The predicted results clearly show the cyclic variations of the blade power and thrust coefficients due to angular inflow. The flow changes from blade passage to passage are illustrated in terms of static pressure contours. The predicted blade surface pressure waveforms are compared with flight measurements. The predictions at the inboard radial station, r/R=0.68, show reasonable agreement with flight data. At the outboard radial station, r/R=0.95, where the interactions of the tip vortex, the tip-region flow and the blade wake appear to result in a complex nonlinear measured response, the prediction shows poor agreement.

14. SUBJECT TERMS	15. NUMBER OF PAGES
Propfan; Aerodynamics; Aeroacoustics	14
	16. PRICE CODE: A03

17. SECURITY CLASSIFICATION OF REPORT	18. SECURITY CLASSIFICATION OF THIS PAGE	19. SECURITY CLASSIFICATION OF ABSTRACT	20. LIMITATION OF ABSTRACT
Unclassified	Unclassified	Unclassified	

PAGE 13 INTENTIONALLY BLANK

PRECEDING PAGE BLANK NOT FILMED